

EEE431 – Computational Assignment 2

Emir Arda Bayer
Digital Communications

Fall 2025

Contents

1 Part I: Binary Antipodal Modulation	2
1.1 Part (a): Signal Space Representation	2
1.2 Part (b): Optimal Receiver and Theoretical SEP	3
1.3 Part (c): Impact of Sampling Period	3
1.4 Part (d)-(e): Simulation Results (Equal Priors)	3
1.5 Part (f): Unequal Priors	5
1.6 Part (g)-(h): MAP vs. ML Performance	5
2 Part II: 4-Symbol Constellations	7
2.1 Part (a): Constellation 1 Analysis	7
2.2 Part (b)-(c): Constellation 1 Results	7
2.3 Part (d): Constellation 2 Comparison	8
2.4 Part (e): Bit Error Rate with Natural Coding	9
2.5 Part (f): Natural vs. Gray Coding Comparison	10

Introduction

This assignment investigates optimal receiver design for binary and M -ary modulation schemes. Part I focuses on a binary antipodal scheme using a parabolic pulse shape. I derive the signal space representation, implement the optimal correlation receiver, and analyze performance under both equal and unequal prior probabilities. Part II explores 4-symbol constellations in 2D signal space. I derive the Union Bound for symbol error probability (SEP) and compare the performance of two distinct constellation geometries. Finally, I analyze the Bit Error Rate (BER) performance of Natural versus Gray coding.

All simulations were performed in MATLAB using Monte Carlo methods with 10^6 realizations to ensure statistical reliability. A fixed random seed was utilized for all simulations to ensure reproducibility.

1 Part I: Binary Antipodal Modulation

1.1 Part (a): Signal Space Representation

The modulation uses a parabolic pulse $p(t) = t(T - t)$ for symbol 0 and $-p(t)$ for symbol 1, with duration $T = 1$. The sampling period was set to $T_s = T/20 = 0.05$.

The energy of the pulse is computed as:

$$E_p = \int_0^T p^2(t) dt \approx \sum_n p[n]^2 T_s.$$

Since the scheme is binary antipodal, the signal space is 1-dimensional. The single orthonormal basis function is:

$$\phi_1(t) = \frac{p(t)}{\sqrt{E_p}}.$$

Figure 1 displays the signal waveforms and the resulting basis function.

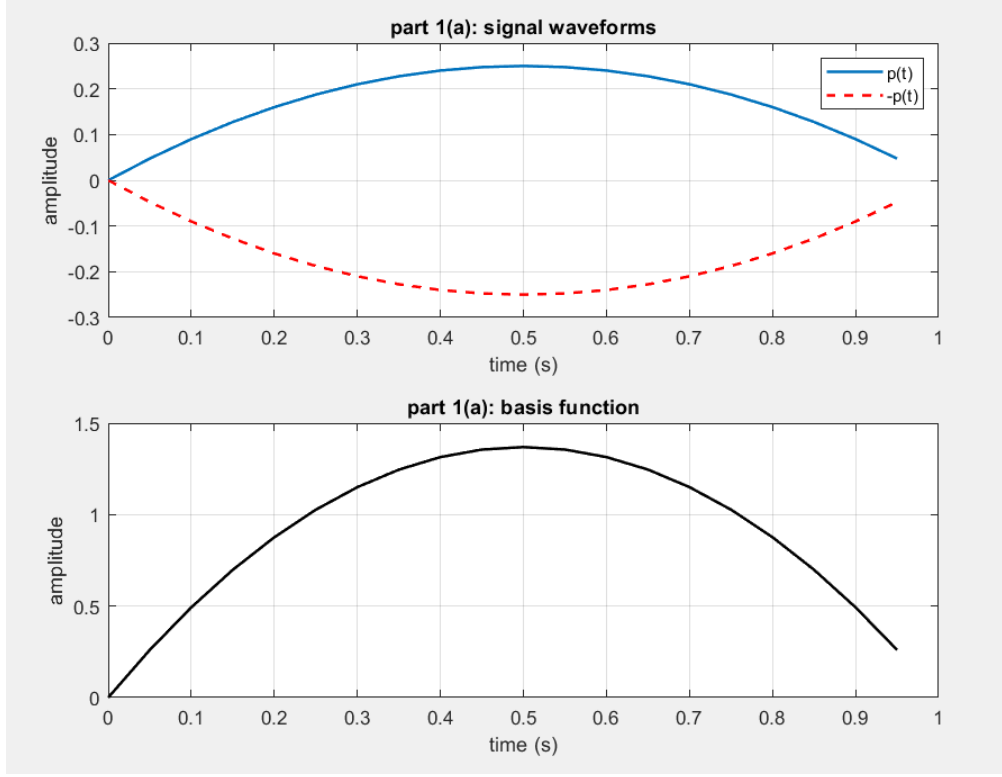


Figure 1: Part 1(a): Signal waveforms $p(t)$, $-p(t)$ and basis function $\phi_1(t)$.

1.2 Part (b): Optimal Receiver and Theoretical SEP

The received signal is $r(t) = s_m(t) + n(t)$. The sufficient statistic r is obtained by projecting $r(t)$ onto $\phi_1(t)$. For equal priors, the Maximum Likelihood (ML) decision rule is:

$$\text{Decide } s_0 \text{ if } r > 0, \quad \text{Decide } s_1 \text{ if } r < 0.$$

The theoretical probability of error is derived by considering the noise distribution. Given s_0 (mapped to $+\sqrt{E_s}$) is sent, an error occurs if the noise component $n < -\sqrt{E_s}$. Since $n \sim \mathcal{N}(0, N_0/2)$:

$$P_e = P(n < -\sqrt{E_s}) = \int_{-\infty}^{-\sqrt{E_s}} \frac{1}{\sqrt{\pi N_0}} e^{-\frac{x^2}{N_0}} dx = Q\left(\sqrt{\frac{2E_s}{N_0}}\right).$$

1.3 Part (c): Impact of Sampling Period

The power spectral density of the noise, N_0 , is a physical parameter independent of the sampling rate. In the discrete simulation, the variance of the additive noise samples scales as $\sigma^2 = \frac{N_0}{2T_s}$. Thus, the effective SNR remains invariant to the sampling period provided T_s is sufficient to avoid aliasing.

1.4 Part (d)-(e): Simulation Results (Equal Priors)

The simulation was performed for γ_s ranging from -10 dB to 9 dB. Figure 2 shows the estimated SEP on a linear scale, while Figure 3 compares these results to the theoretical curve on a logarithmic scale. The simulation matches the theory perfectly.

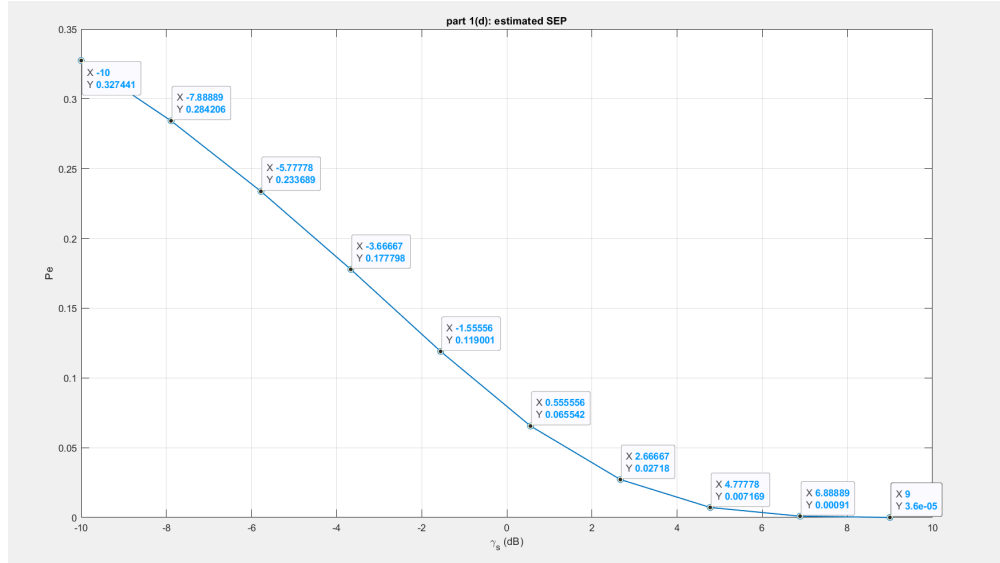


Figure 2: Part 1(d): Estimated SEP vs γ_s (Linear Scale).

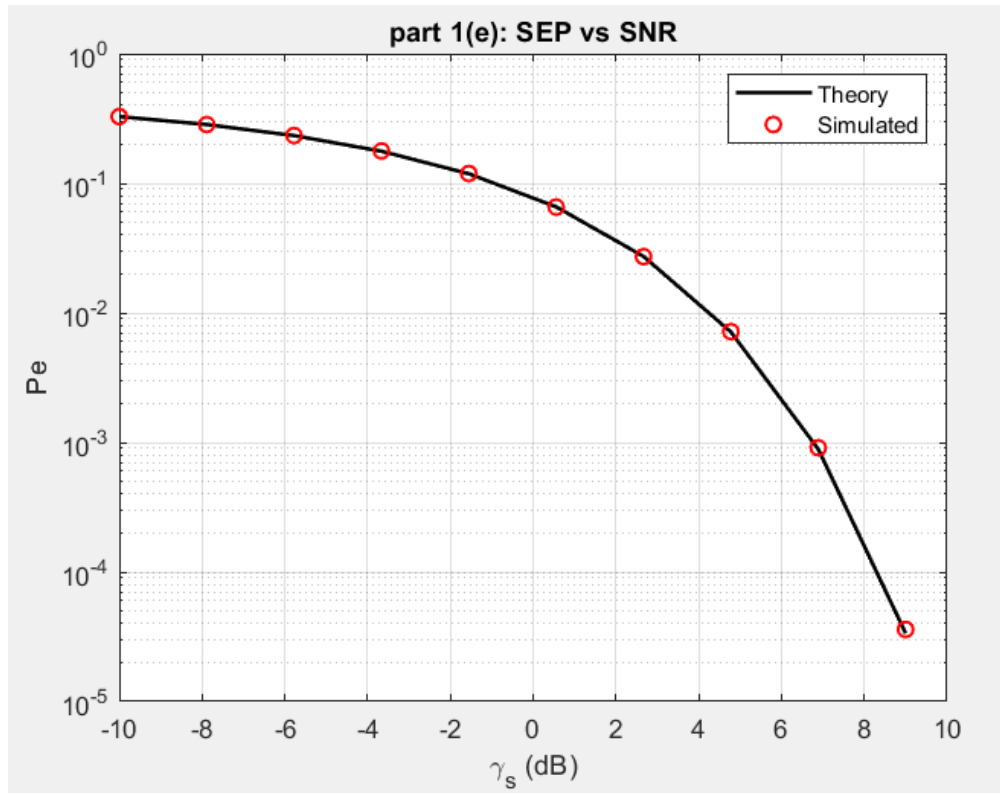


Figure 3: Part 1(e): Theoretical vs. Simulated SEP (Log Scale).

1.5 Part (f): Unequal Priors

With $P(s_1) = 0.25$ and $P(s_0) = 0.75$, the ML receiver is suboptimal. The Maximum A Posteriori (MAP) rule shifts the decision threshold η to favor the more probable symbol s_0 :

$$\eta = \frac{N_0}{4\sqrt{E_p}} \ln \left(\frac{P(s_1)}{P(s_0)} \right).$$

1.6 Part (g)-(h): MAP vs. ML Performance

Figure 4 shows the MAP receiver's estimated SEP. Figure 5 compares the MAP receiver against the ML receiver. The MAP receiver yields a lower probability of error at low SNR where the prior information significantly aids the decision. As SNR increases, the likelihood ratios dominate the decision rule, diminishing the impact of the prior probabilities. Consequently, the MAP and ML performance curves converge at high γ_s .

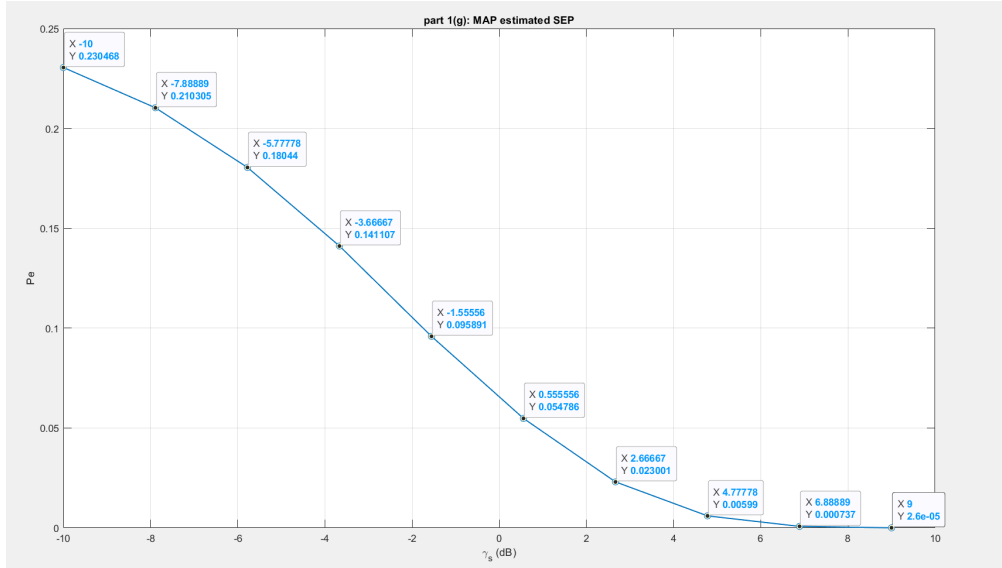


Figure 4: Part 1(g): MAP Estimated SEP (Linear Scale).

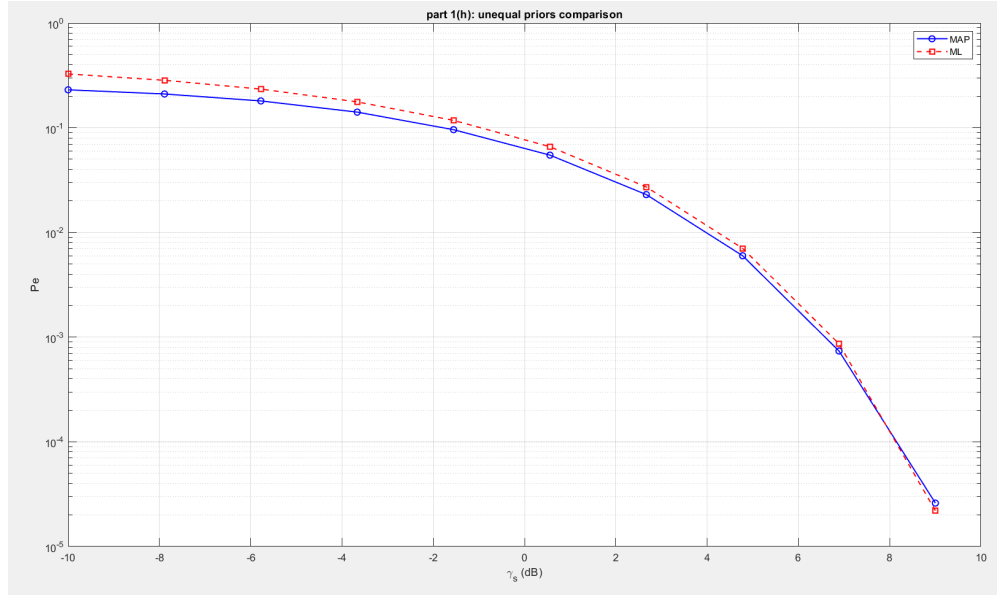


Figure 5: Part 1(h): Comparison of MAP and ML receivers.

2 Part II: 4-Symbol Constellations

2.1 Part (a): Constellation 1 Analysis

The first constellation is defined by symbols $s_1 = [A, A]$, $s_2 = [A, -A]$, $s_3 = [-A, -A]$, $s_4 = [-A, 0]$ with $A = \sqrt{4/7}$. The Union Bound approximates the total SEP by summing the pairwise error probabilities. The pairwise error probability between s_i and s_j depends on the noise projection exceeding half the Euclidean distance $d_{ij} = \|s_i - s_j\|$:

$$P(s_i \rightarrow s_j) = P\left(n > \frac{d_{ij}}{2}\right) = Q\left(\frac{d_{ij}}{\sqrt{2N_0}}\right).$$

Summing over all distinct pairs yields the bound:

$$P_e \leq \frac{1}{M} \sum_{i=1}^M \sum_{j \neq i} Q\left(\frac{\|s_i - s_j\|}{\sqrt{2N_0}}\right).$$

2.2 Part (b)-(c): Constellation 1 Results

Figure 6 displays the simulated SEP on a linear scale. Figure 7 demonstrates the convergence of the simulation to the Union Bound at high SNR. The bound is loose at low SNR because the pairwise error events are not mutually exclusive. At high SNR, the nearest-neighbor error events dominate, making the union bound asymptotically tight.

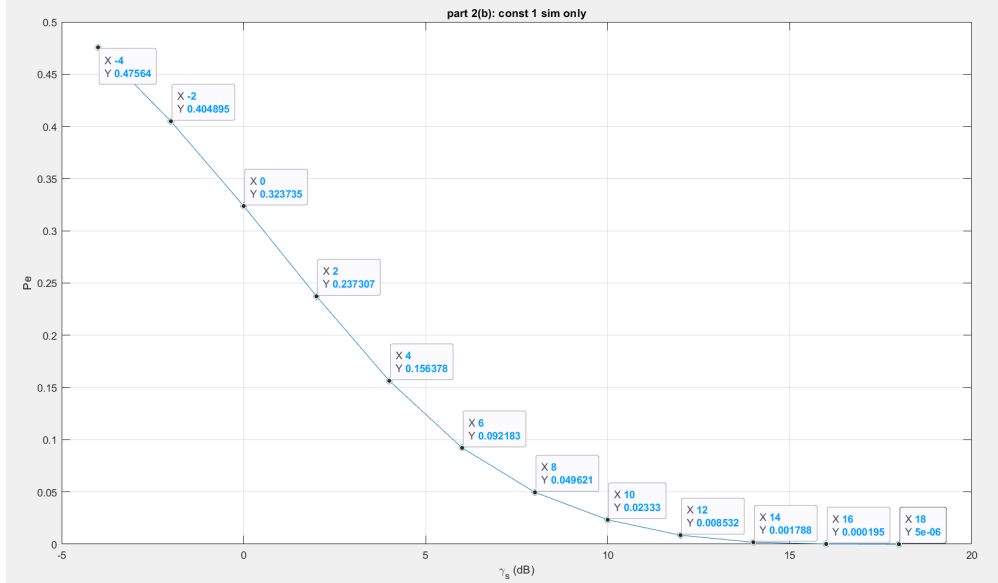


Figure 6: Part 2(b): Constellation 1 Estimated SEP (Linear Scale).

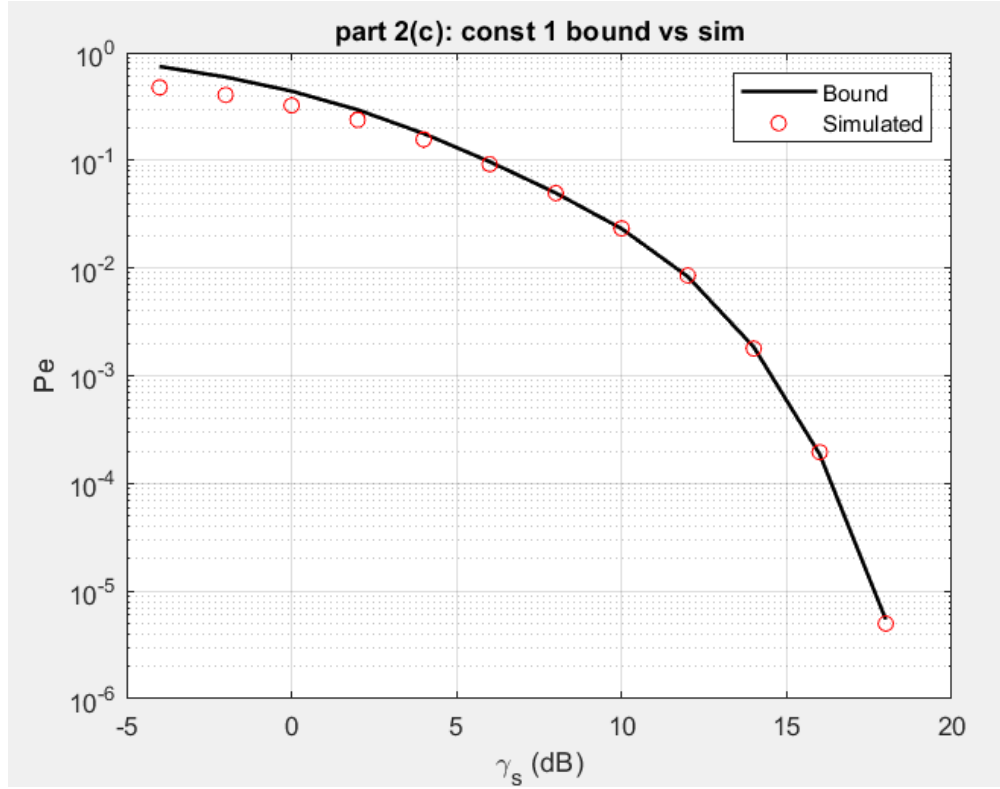


Figure 7: Part 2(c): Constellation 1 Union Bound vs. Simulation.

2.3 Part (d): Constellation 2 Comparison

Constellation 2 ($s_4 = [-A, A]$, $A = \sqrt{1/2}$) forms a square geometry. Figure 8 compares the two constellations, showing Constellation 2 outperforms Constellation 1 due to a larger minimum Euclidean distance. Figure 9 validates the Constellation 2 simulation against its specific Union Bound.

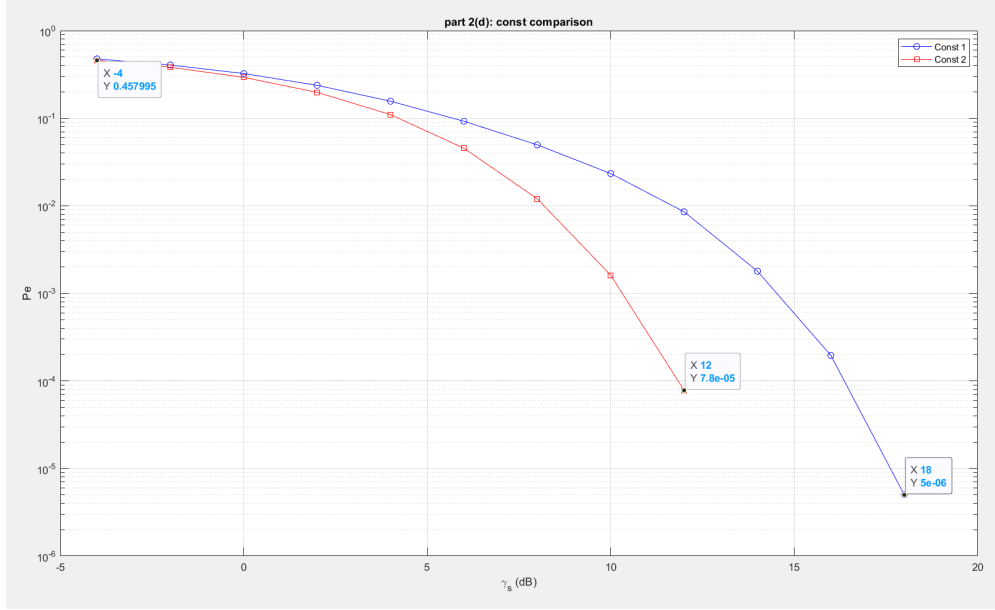


Figure 8: Part 2(d): Performance comparison of Constellation 1 and 2.

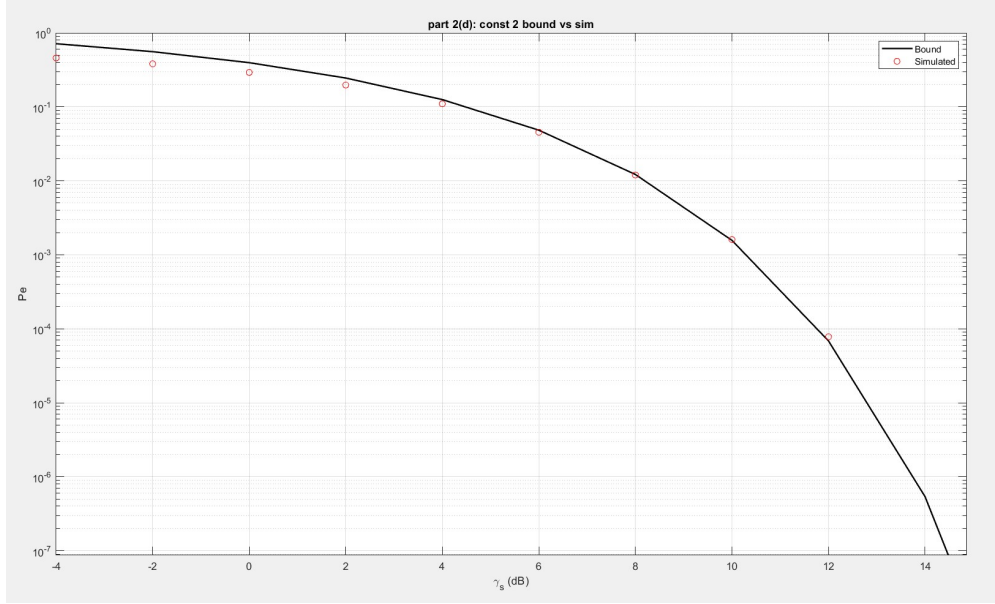


Figure 9: Part 2(d): Constellation 2 Union Bound vs. Simulation.

2.4 Part (e): Bit Error Rate with Natural Coding

I computed the Bit Error Probability (BER) for Constellation 2 using Natural coding. Figure 10 shows the BER decreasing linearly on a logarithmic scale.

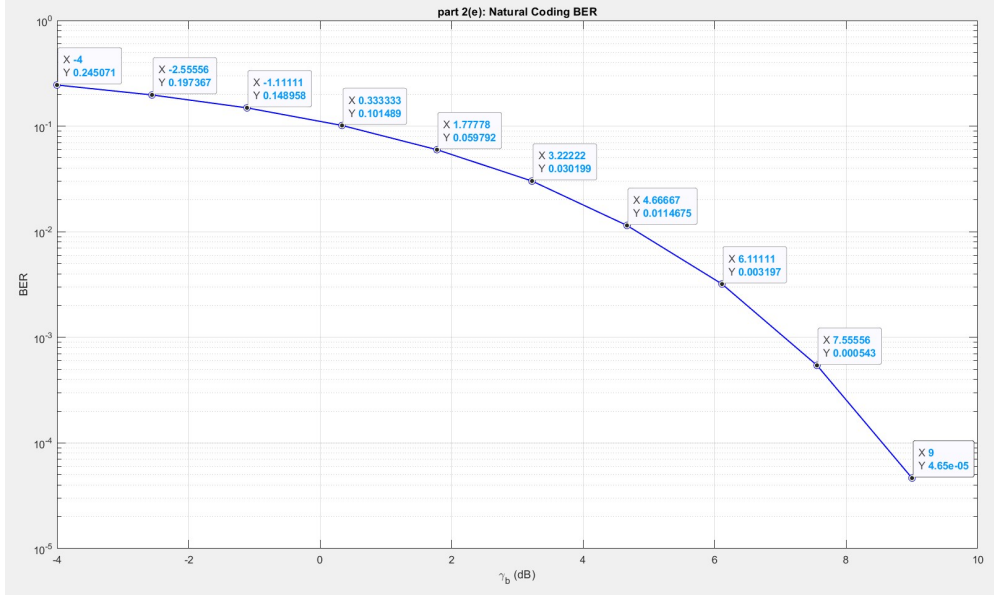


Figure 10: Part 2(e): BER for Constellation 2 using Natural Coding.

2.5 Part (f): Natural vs. Gray Coding Comparison

Figure 11 compares Natural coding with Gray coding. Gray coding minimizes bit errors by ensuring nearest neighbors differ by only 1 bit, yielding superior performance.

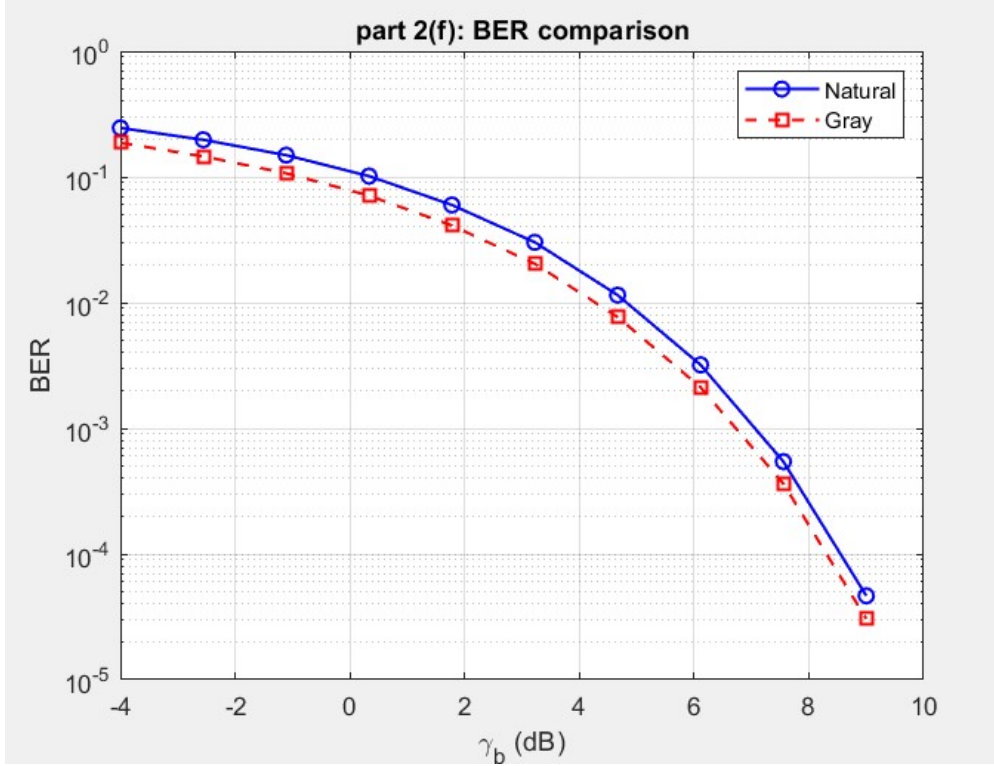


Figure 11: Part 2(f): BER comparison for Natural and Gray coding.

Conclusion

In Part I, I demonstrated that the optimal receiver for a known signal in AWGN is the correlation receiver. The simulation results validated the theoretical error probability. Furthermore, the results confirmed that when symbol probabilities are unequal, the MAP receiver outperforms the ML receiver.

In Part II, the geometry of the signal constellation proved critical. Constellation 2 (square) outperformed Constellation 1 because it utilized the signal space more efficiently. Finally, the BER analysis verified that Gray coding minimizes bit errors by mapping adjacent symbols to Hamming distance 1.

References

- Lecture notes for EEE431, Fall 2025.